Superhydrophobicity of 3D Porous Copper Films Prepared Using the Hydrogen Bubble Dynamic Template

Ying Li, Wen-Zhi Jia, Yan-Yan Song, and Xing-Hua Xia*

The Key Laboratory of Analytical Chemistry for Life Science, School of Chemistry and Chemical Engineering, Nanjing University, Nanjing 210093, China

Received July 2, 2007. Revised Manuscript Received September 3, 2007

We have successfully sculptured a variety of copper films with open interconnected macroporous walls and nanoparticles using hydrogen bubbles as the dynamic template. In this process, the hydrogen bubbles arising from the electrochemical reduction of H^+ in the deposition process functioned as the dynamic template for metal electrodeposition. Cu was electrodeposited and grew within the interstitial spaces between the hydrogen bubbles to form a macroporous film of Cu nanoparticles on the substrate, showing a typical integration of micro−nanostructure. The pore diameters and wall thickness of the porous copper films were successfully tailored by adjusting the concentration of the electrodeposition electrolyte, the applied current density, and the concentration of the surfactant (cetyltrimethylammonium bromide, CTAB). Water contact angle measurements showed that the hydrophobicity of the prepared porous structures could be tuned by changing the pore size and wall thickness.

Introduction

Because of extremely large specific surface areas for charge and mass transport in electrochemistry, three-dimensionally (3D) porous materials are important for both academic study and technological applications in catalysts,[1−3] separation systems,[4,5] batteries,[6,7] sensors,[8] and electronic materials.[9] The most popular approach for the preparation of the porous materials with controlled characteristics is the template-directed synthesis method, in which a disposable hard template is used to deposit other new materials in its interstitial spaces. The template can then be removed by combustion or etching. Finally, the new materials with the replica structure of the template are obtained. To date, several kinds of templates have been proposed for the formation of films, membranes, or powders of porous metals with tunable pore sizes and structures, such as porous polycarbonate membranes,[10,11] anodic alumina membranes,[12−15] colloidal crystals,[16−18] and echinoid skeletal structures.[19]

Recently, a new green and promising template, gas bubble dynamic template, was proposed, by which self-supported 3D porous metals[20−22] (Ni, Cu, Sn) and alloys[23] (Cu_6Sn_5) with highly porous dendritic walls and numerous nanoparticles have been successfully prepared from electrochemical deposition processes. As shown in Scheme 1, hydrogen bubbles arising from the electrochemical reduction of H^+ functioned as the dynamic template for metal electrodeposition. Metal was electrodeposited and grew within the interstitial spaces between the hydrogen bubbles and formed a macroporous film of metallic nanoparticles on the substrate. We used this approach followed by a galvanic replacing process to fabricate 3D macroporous gold films that showed enhanced electrocatalytic activity toward the oxidation of glucose.[24] Compared with hard templates, the hydrogen bubble templates possess several advantages: low cost, ease of preparation, facile control of structure, and facile one-step synthesis process, including preparation of the template, metal deposition, and elimination of the template.

* Corresponding author. E-mail: xhxia@nju.edu.cn (X.H.X.). Tel/fax: 86 25 83597436.

(1) Zhang, C. X.; Babonneau, F.; Bonhomme, C.; Laine, R. M.; Soles, C. L.; Hristov, H. A.; Yee, A. F. *J. Am. Chem. Soc.* **1998**, *120*, 8380.
(2) Chai, G. S.; Yoon, S. B.; Yu, J. S.; Choi, J. H.; Sung, Y. E. *J. Phys. Chem. B* **2004**, *108*, 7074.
(3) Yu, J. S.; Kang, S.; Yoon, S. B.; Chai, G. S. *J. Am. Chem. Soc.* **2002**, *124*, 9382.
(4) Kusakabe, K.; Kuroda, T.; Murata, A.; Morooka, S. *Ind. Eng. Chem. Res.* **1997**, *36*, 649.
(5) Magoulianti, E.; Beltsios, K.; Davazoglou, D.; Kanellopoulos, N. *J. Phys. IV* **2001**, *11*, 1191.
(6) Yuan, L.; Guo, Z. P.; Konstantinov, K.; Liu, H. K.; Dou, S. X. *J. Power Sources* **2006**, *159*, 345.
(7) Paula, R. M.; Pallone, E. M. J. A.; Neves, S. *Electrochim. Acta* **2006**, *51*, 6419.
(8) Zhang, G. Y.; Li, C. S.; Cheng, F. Y.; Chen, J. *Sens. Actuators B* **2007**, *120*, 403.
(9) Hu, Y. S.; Guo, Y. G.; Sigle, W.; Hore, S.; Balaya, P.; Maier, J. *Nat. Mater.* **2006**, *5*, 713.
(10) Guo, Y. L.; Yui, H.; Minamikawa, H.; Yang, B.; Masuda, M.; Ito, K.; Shimizu, T. *Chem. Mater.* **2006**, *18*, 1577.
(11) Kazeminezhad, I.; Barnes, A. C.; Holbrey, J. D.; Seddon, K. R.; Schwarzacher, W. *Appl. Phys. A* **2007**, *86*, 373.
(12) Yuan, J. H.; He, F. Y.; Sun, D. C.; Xia, X. H. *Chem. Mater.* **2004**, *16*, 1841.
(13) Yuan, J. H.; Wang, K.; Xia, X. H. *Adv. Funct. Mater.* **2005**, *15*, 803.
(14) Qiu, J. D.; Peng, H. Z.; Liang, R. P.; Li, J.; Xia, X. H. *Langmuir* **2007**, *4*, 2133.
(15) Chen, W.; Yuan, J. H.; Xia, X. H. *Anal. Chem.* **2005**, *77*, 8102.
(16) Song, Y. Y.; Zhang, D.; Xia, X. H. *Chem.−Eur. J.* **2005**, *11*, 2177.
(17) Wang, C. H.; Yang, C.; Song, Y. Y.; Gao, W.; Xia, X. H. *Adv. Funct. Mater.* **2005**, *15*, 1267.
(18) Chen, W.; Xia, X. H. *Chem. Phys. Chem.* **2007**, *8*, 1009.
(19) Meldrum, F. C.; Seshadri, R. *Chem. Commun.* **2000**, *1*, 29.
(20) Shin, H. C.; Liu, M. L. *Chem. Mater.* **2004**, *16*, 5461.
(21) Shin, H. C.; Dong, J.; Liu, M. L. *Adv. Mater.* **2004**, *16*, 237.
(22) Shin, H. C.; Dong, J.; Liu, M. L. *Adv. Mater.* **2003**, *15*, 1610.
(23) Shin, H. C.; Liu, M. L. *Adv. Funct. Mater.* **2005**, *15*, 582.
(24) Li, Y.; Song, Y. Y.; Yang, C.; Xia, X. H. *Electrochem. Commun.* **2007**, *9*, 981.
(25) Zhao, Y. H.; Masuoka, T.; Tsuruta, T. *Int. J. Heat Mass Transfer* **2002**, *45*, 3189.

10.1021/cm071738j CCC: $37.00
Published on Web 10/10/2007

Scheme 1. Schematic Illustration of the Experimental Procedure That Generates Porous Copper Film with Open Interconnected Macroporous Walls and Nanoparticles Using the Hydrogen Bubble Dynamic Template-Directed Synthesis Method

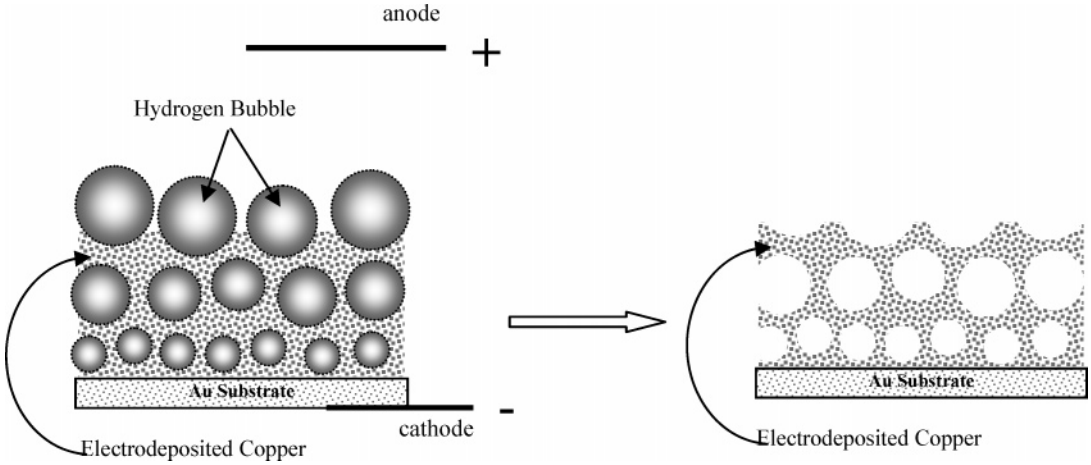

On the basis of the concept of this bubble template-directed synthesis method, it is clear that the pore size and wall thickness of porous metallic films are determined by the bubble size. In this work, we introduced surfactants into this synthesis method to design the deposited metallic film structures. Surfactants have been widely used as stabilizers in aqueous media to alter the surface tension of the sol/gas and protect the bubbles from coalescence; therefore, a highly stable, well-dispersed bubble template can be obtained.[26−33] We took these advantages of the surfactants into the bubble-directed synthesis method to tailor and stabilize the hydrogen bubbles generated from an electrochemical reduction of proton, which subsequently influences the pore structure of the deposited metal films. In addition, the influence of the concentration of electrolyte and surfactant (cetyltrimethylammonium bromide, CTAB) and the deposition current density on the morphology of copper films was investigated. Because Jiang and co-workers demonstrated that the unique self-cleaning property of lotus leaves was due to the cooperation of microstructures and nanostructures on these surfaces,[34−38] we also investigated the self-cleaning property of the copper films that have micro-nano structures.

Experimental Section

Reagents. $CuSO_4$ was purchased from the Shanghai Tingxin Chemical Factory (Shanghai, China). H_2SO_4 was obtained from the Nanjing Chemical Reagents Ltd. (Nanjing, China). CTAB was purchased from the Shanghai Lingfeng Chemical Reagents Ltd. (Shanghai, China). All the chemicals used in this investigation were of analytic grade. All solutions were prepared with deionized water (>18 MΩ, PureLab Classic Corp.).

Electrochemical Experiments. The electrochemical experiments were carried out on a CHI 1140A electrochemical workstation (CH Instrument). A traditional three-electrode system with a platinum mesh as the auxiliary electrode, a saturated calomel electrode (SCE), or reversible hydrogen electrode (RHE) as the reference electrode, and a gold disk electrode (8.0 mm diameter) as the working electrode was employed. All potentials in this paper refer to the SCE reference electrode.

Prior to use, the polycrystalline Au disk electrode (substrate) was polished consecutively with 1, 0.3, and 0.05 μm alumina powders and sonicated in water for 5 min. The well-polished electrode was then electrochemically pretreated by cycling the potential between −0.2 and +1.6 V in a solution of H_2SO_4 (0.5 M) at a scan rate of 0.10 V s^{-1} until a stable voltammogram was obtained. The current density in this work was reported as the ratio of current to geometrical surface area of the electrode (0.5 cm^2).

Preparation of Macroporous Cu Films. The pretreated gold electrode was used as the working electrode (substrate) for copper deposition. The distance between the anode and cathode was kept at 0.5 cm. To investigate the effect of the electrolyte and the current density on the microstructures of the porous copper films, we employed various concentrations of electrolyte and different applied current densities. Different concentrations of CTAB (from 10 μM to 5 mM) were then added to 0.4 M $CuSO_4$ and 0.5 M H_2SO_4 to tailor and stabilize the evolved hydrogen bubbles. Deposition was performed in a stationary electrolyte solution (without stirring or N_2 bubbling). All the experiments were repeated at least three times, and reproducible results were obtained. All the measurements were carried out at room temperature (20 ± 1 °C).

Methods. Scanning electron microscopy (SEM) measurements were performed on a JEOL JSM-6360-LV scanning electron microscope. Surface modification was carried out by immersing the as-prepared substrates in an ethanol solution of *n*-hendecanethiol (1×10^{-3} M) overnight and then washing them in turn with ethanol and water and dried with nitrogen. The static contact angles of the as-prepared surfaces were measured with a commercial instrument (OCA 20, DataPhysics Instruments GmbH, Filderstadt). A distilled water droplet (drop volume 10 μL) was used as the indicator in the experiment to characterize the wetting property of the as-prepared self-cleaning surfaces.

(26) Wang, L. G.; Yoon, R. H. *Colloids Surf., A* **2006**, *282*, 84.
(27) Melo, F.; Laskowski, J. S. *Miner. Eng.* **2006**, *19*, 766.
(28) Grau, R. A.; Laskowski, J. S.; Heiskanen, K. *Int. J. Miner. Process.* **2005**, *76*, 225.
(29) Aldrich, C.; Feng, D. *Miner. Eng.* **2000**, *13*, 1049.
(30) Laskowski, J. S.; Tlhone, T.; Williams, P.; Ding, K. *Int. J. Miner. Process.* **2003**, *72*, 289.
(31) Bhakta, A.; Ruckenstein, E. *Adv. Colloid Interface Sci.* **1997**, *70*, 1.
(32) Cho, Y. S.; Laskowski, J. S. *Int. J. Miner. Process.* **2002**, *64*, 69.
(33) Danov, K. D.; Valkovska, D. S.; Kralchevsky, P. A. *J. Colloid Interface Sci.* **2003**, *267*, 243.
(34) Gao, X. F.; Jiang, L. *Nature* **2004**, *432*, 36.
(35) Sun, T. L.; Feng, L.; Gao, X. F.; Jiang, L. *Acc. Chem. Res.* **2005**, *38*, 644.
(36) Feng, L.; Li, S. H.; Li, Y. S.; Li, H. J.; Zhang, L. J.; Zhai, J.; Song, L. Y.; Liu, B. Q.; Jiang, L.; Zhu, D. B. *Adv. Mater.* **2002**, *14*, 1857.
(37) Zhang, X.; Shi, F.; Yu, X.; Liu, H.; Fu, Y.; Wang, Z. Q.; Jiang, L.; Li, X. Y. *J. Am. Chem. Soc.* **2004**, *126*, 3064.
(38) Wang, S. T.; Feng, L.; Liu, H.; Sun, T. L.; Zhang, X.; Jiang, L.; Zhu, D. B. *Chem. Phys. Chem.* **2005**, *6*, 1475.

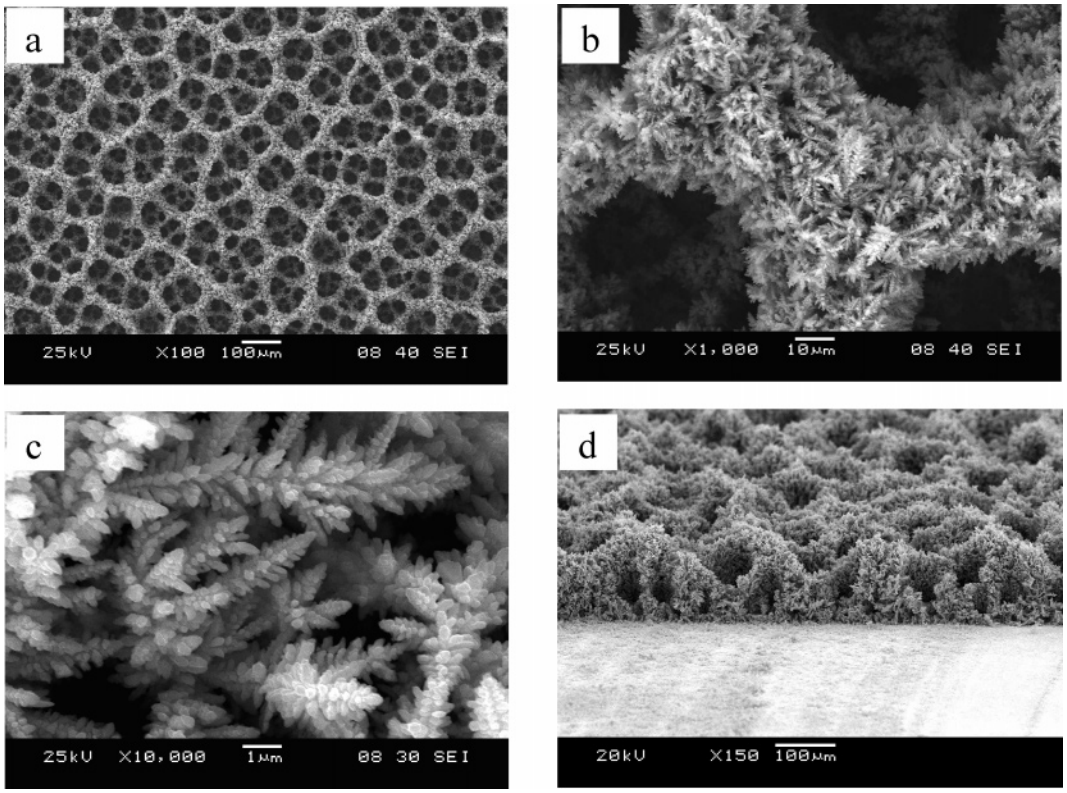

Figure 1. Top-view and side-view SEM images with different magnifications of the porous Cu film electrochemically deposited at a 0.8 A cm^{-2} cathodic current density in a solution of 0.1 M $CuSO_4$ and 0.5 M H_2SO_4 for 45 s.

Results and Discussion

Preparation of 3D Porous Copper Films by Hydrogen Bubble Dynamic Template. Figure 1 displays some typical SEM images of the porous copper films electrochemically deposited at a 0.8 A cm^{-2} cathodic current density in a 0.1 M $CuSO_4$ and 0.5 M H_2SO_4 solution for 45 s. It is clear that the copper films are of 3D interconnected porous structures. Magnified SEM images (images b and c in Figure 1) show that the porous structure consisted of numerous dendrites in all directions, which construct the pore walls, forming a mechanically self-supported film. The feature size of the pores in the copper film is about 100 μm (Figure 1a). Because the overpotential at the gold substrate for hydrogen evolution is lower than the newly electrodeposited copper in a highly acidic media, the hydrogen bubbles evolved mostly from the surface of the gold substrate. Where there is a hydrogen bubble, there will be no deposition of copper because there are no copper ions available. The growth of copper toward the hydrogen bubble is inhibited, leading to copper deposition only at the interstices of hydrogen bubbles. Thus, the numerous hydrogen bubbles evolving at different locations on the substrate create the pores in the copper films during the electrodeposition process. In other words, the hydrogen bubbles function as a dynamic template for copper deposition. Although most of the current leads to the formation of hydrogen bubble at the gold surface, there is still a partial current directed to the formation of hydrogen at freshly deposited copper surface. This slowly formed small amount hydrogen results in the formation of highly nanoporous wall of the copper films. As seen from Figure 1, the pore size of the copper film increases with the distance away from the substrate because of the coalescence of hydrogen bubbles, creating structures ideally suited for fast transport of electroactive gas/ion through the porous films, which can also be seen from the side view SEM image of the porous structures (Figure 1d). On the contrary, the conventional 3D porous materials with uniform pore size is not ideally suited for fast electrochemical reactions because the small pores near the top surface may restrict the transport of electroactive species (gas/ion) to the inner space of the structure, leading to low utilization of the whole surface area because of mass transport limitations.[20−23] In addition, the prepared porous copper films in our work can maintain their porous structure

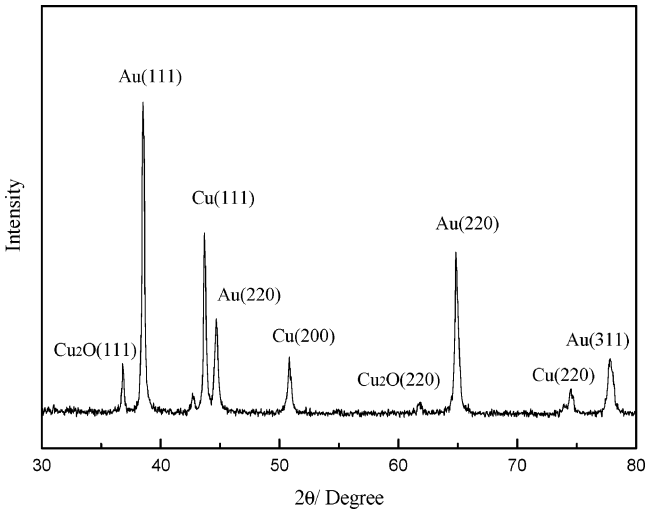

Figure 2. Typical XRD pattern of the as-prepared macroporous copper film.

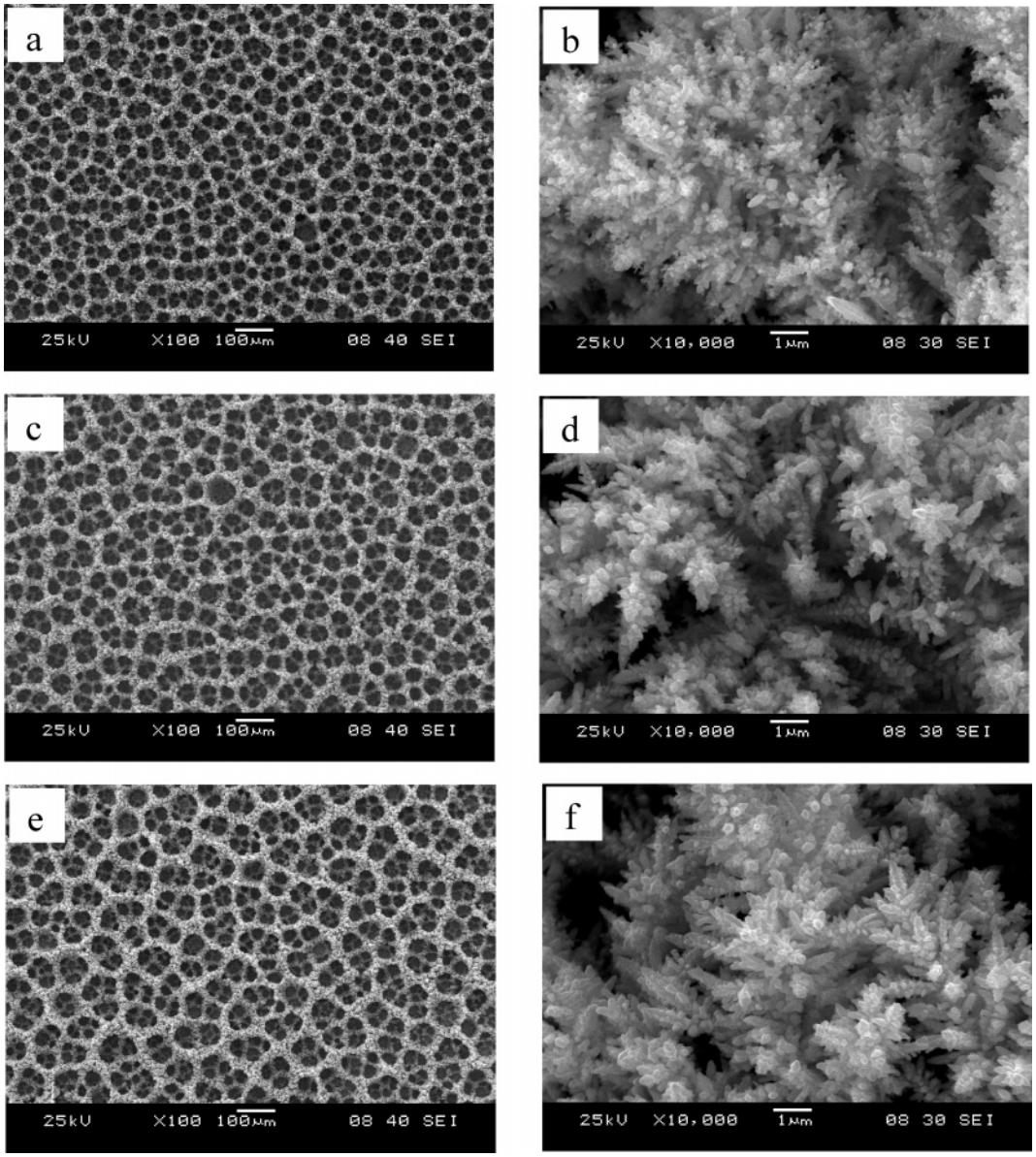

Figure 3. SEM images of porous copper films created by electrodeposition at a 0.8 A cm^{-2} cathodic current density in 0.5 M H_2SO_4 and different $CuSO_4$ concentrations. (a,b) 0.04 M $CuSO_4$; (c,d) 0.06 M $CuSO_4$; (e,f) 0.08 M $CuSO_4$.

during handling in electrolyte and subsequent procedures for drying and characterization.

Figure 2 shows the typical XRD pattern of the as-prepared macroporous copper film. The characteristics of the face-centered cubic (fcc) copper crystal structure is evident as indicated by the orientations along the Cu(111), Cu(200), and Cu(220) directions. The average particle size of the deposited copper was calculated to be approximately 32 nm from a (111) X-ray diffraction peak of the copper fcc lattice in terms of the Scherrer equation. These small particles aggregate to form large nodules (about 3 μm in size, see Figure 1). In addition, small Cu_2O peaks were identified from the XRD pattern. Cu_2O diffraction is due to the oxide formation on the copper surface in the air. Because of the abundant protons in the electrolyte, the growing copper tips always experience the highly acidic atmosphere around them, which suppresses the oxide formation and enhances the reduction of copper to metallic copper.[20] It is clear that the feature peak of the gold in the X-ray diffraction pattern is caused by the gold substrate.

Reduction of Pore Size of the Porous Copper Films. The electrodeposition conditions including solution composition and cathodic current considerably influence the pore size and the wall thickness of the resulted porous copper films. In the present method, the porous structure of the copper films is caused by the competitive reaction of copper deposition and hydrogen evolution. An increase in the evolution rate of hydrogen bubbles would influence the porous structure (i.e., the surface pore size and the wall thickness). First, the influence of electrolyte concentration of copper sulfate on the porous structure of the deposited copper films was studied. Under constant current deposition conditions, with the increase in copper sulfate concentration, the partial current due to the electrochemical reduction of copper ions will increase; in contrast, the partial current due to the hydrogen evolution decreases. Figure 3 shows the SEM

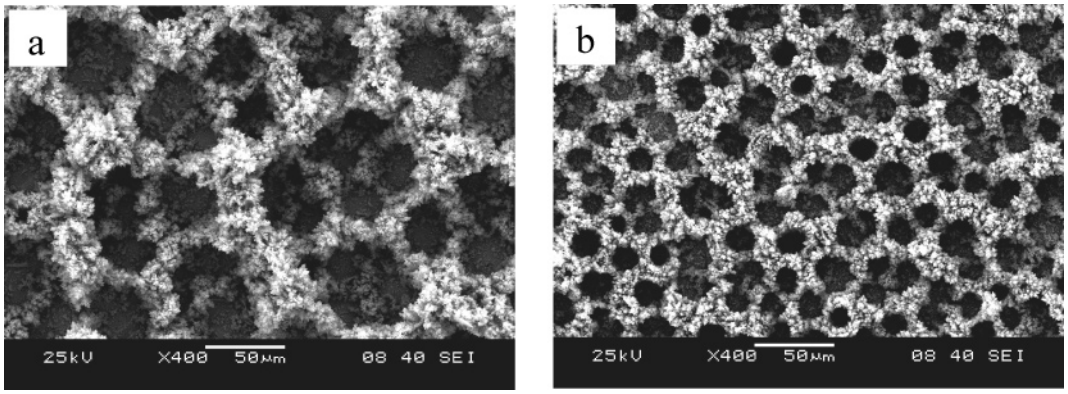

Figure 4. SEM images of porous copper films electrodeposited at current density of (a) 0.4 or (b) 1.2 A cm^{-2} in a solution of 0.04 M $CuSO_4$ + 0.5 M H_2SO_4.

images of the copper films deposited from electrolytes with different concentration of $CuSO_4$. As expected, the pore size and wall thickness of the porous copper films considerably increase with the $CuSO_4$ concentration. The pore size increases from 40 to 100 μm and the wall thickness increases from 20 to 60 μm as the concentration of copper ion increases from 0.04 to 0.08 M. However, from the XRD results (not shown), the copper particle size does not change very much with the concentration of copper ion.

The lifetime of gas bubbles in solution is controlled by the whole process of the bubble nucleation, growth, collision and coalescence, departure from the substrate surface, and then rupture. The number of hydrogen bubbles increases with the hydrogen evolution rate, which will vigorously agitate the solution near the electrode surface. Therefore, the driving force to remove the hydrogen bubbles from the electrode surface increases with the bubble formation rate because of the increased convection in electrolyte.[25] So a higher evolution rate of hydrogen bubbles results in the formation of smaller bubble size leaving from the substrate surface. Because the pore size of the porous copper film reflects the bubble template, the pore sizes of the porous copper films become smaller. This is consistent with the result in Figure 2a, in which the hydrogen formation rate should be the fastest in Figure 2 because the concentration of copper ion was the lowest.

In addition, we found that the well-defined porous copper films with ramified walls were created in a concentration range of copper ions from 0.04 to 0.1 M Cu^{2+} ions. When the concentration of Cu^{2+} ions was higher than 0.15 M, the pores disappeared completely. This phenomenon can be due to the fact that the evolution rate of hydrogen is too low; the formed hydrogen is too insufficient to act as a dynamic template for copper deposition.

Second, the H_2 evolution rate increases with the increase of applied current density, which produces more vigorous turbulence of electrolyte around the evolved hydrogen bubbles. This will increase the driving force for bubbles departure from the surface of the electrode, resulting in the formation of smaller bubbles as well[25] and thus decreased pore sizes of the porous copper films. Besides the faster formation rate of hydrogen bubble, the deposition rate of copper also increases, which will result in reduced wall thickness. Figure 4 shows the typical SEM images of the porous copper films electrodeposited at different current density. The pore size and wall width of the porous copper films are listed in Table 1. As expected, the size of pores and the wall thickness decrease with increasing applied current density. The average pore size and average wall width of the copper film decreased from 150 and 65 μm at an electrolyzing current density of 0.1 A cm^{-2} to 50 and 25 μm at a deposition current density of 1.2 A cm^{-2}, respectively.

Table 1. Summary of Measured Pore Size and Wall Width of the Porous Copper Films Deposited Electrochemically in the Electrolyte of 0.1 M $CuSO_4$ + 0.1 M H_2SO_4 at Different Applied Current Density

current density (A cm^{-2})	average pore size (μm)	average wall width (μm)
0.1	150	65
0.2	120	50
0.4	110	40
0.8	100	30
1.2	50	25

Table 2. Summary of Measured Pore Size and Wall Width of the Porous Copper Films Electrochemically Deposited from Solutions of 0.04 M $CuSO_4$ + 0.1 M H_2SO_4 Containing Different Concentration of Surfactant

C_{CTAB}	average pore size (μm)	average wall width (μm)
10 μm	40	20
50 μm	35	16
0.1 mM	30	13
0.5 mM	23	9
1 mM	10	6
2 mM	10	6

It has been discussed in the introduction section that the surfactant can both stabilize the bubble system and decrease the surface tension of the bubbles, but the effect of surface tension on the bubble size is trivial.[24−27] Most importantly, the surfactant suppresses the coalescence of the bubble template, which will lead to the formation of bubbles with smaller size. In solution, surfactant adsorbs on the interface between gas and liquid phase, that is, the surfactant adsorbs on the bubbles' surface. It inhibits the collision among the bubbles and blocks the coalescence among the bubbles. The bubble size is then kept small. At low concentration of surfactant, the bubble size should be sensitive to the surfactant concentration. A higher concentration of the surfactant results in the formation of smaller bubbles. When the surfactant concentration exceeds the critical micelle

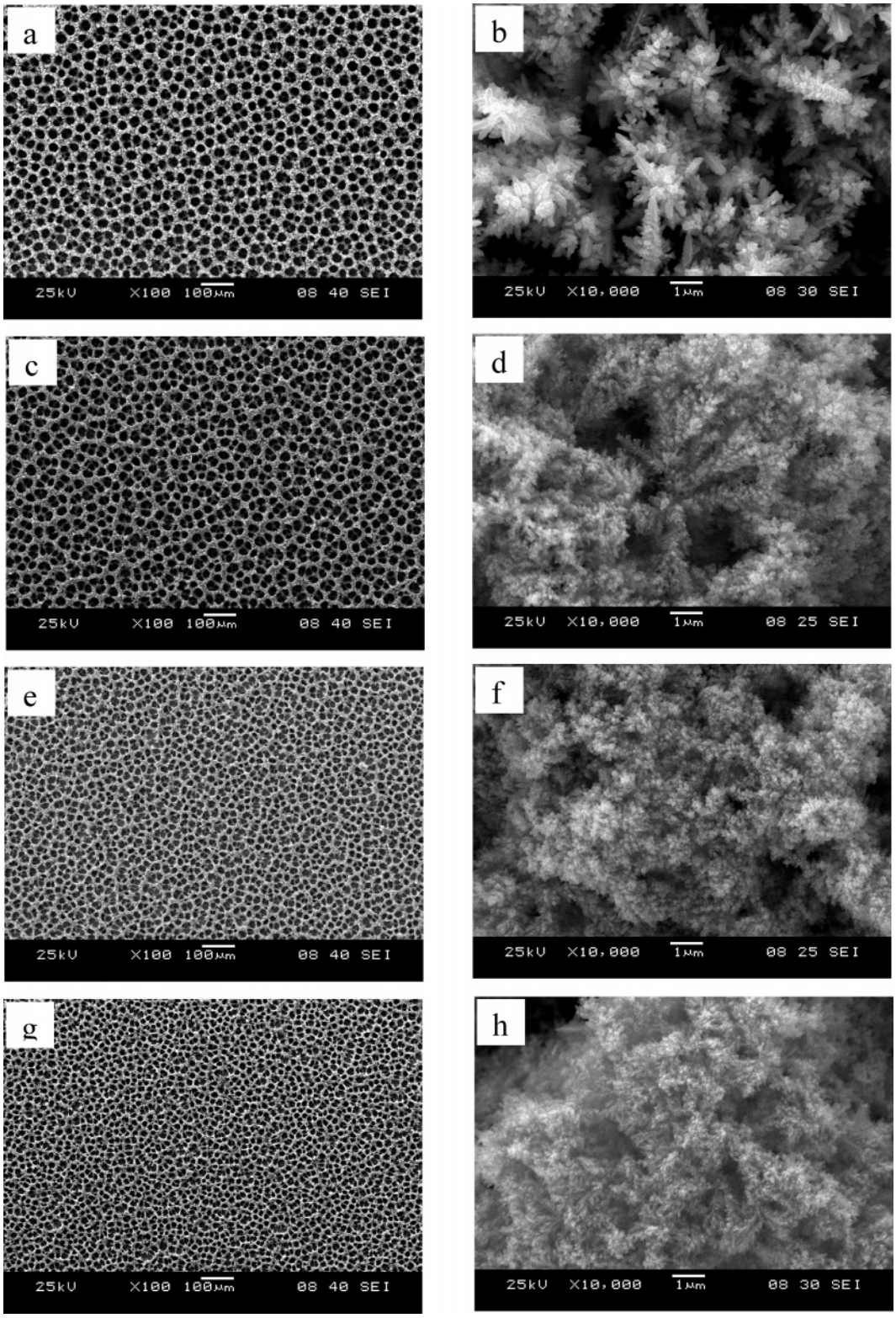

Figure 5. SEM images of porous copper electrodeposited at a 0.8 A cm^{-2} cathodic current density for 85 s in the electrolyte of (a, b) 0.04 M $CuSO_4$ + 0.5 M H_2SO_4 + 0.1 mM, (c, d) 0.5 mM, (e, f) 1 mM, (g, h) and 2 mM CTAB.

concentration (CMC), the surfactant is prone to forms micelles. This would inhibit the surfactant adsorbing on the surface of the hydrogen bubbles. So the bubble size will not be reduced further.[26−33]

We selected CTAB (cationic surfactant) as a model system to investigate the influence of the concentration on the pore size and pore wall thickness of the deposited copper films. The results are shown in Figure 5. When the surfactant concentration was lower than 1 mM, the pore size of the porous copper films decreased with the surfactant concentration increasing. When 1 mM CTAB was added in the solution, the average pore size of the porous copper film was about 10 μm and the wall thickness was 6 μm, which were much smaller than those obtained under the same conditions but without CTAB (Figure 2a). When the CTAB concentration exceeded 1 mM, the pore size and the wall

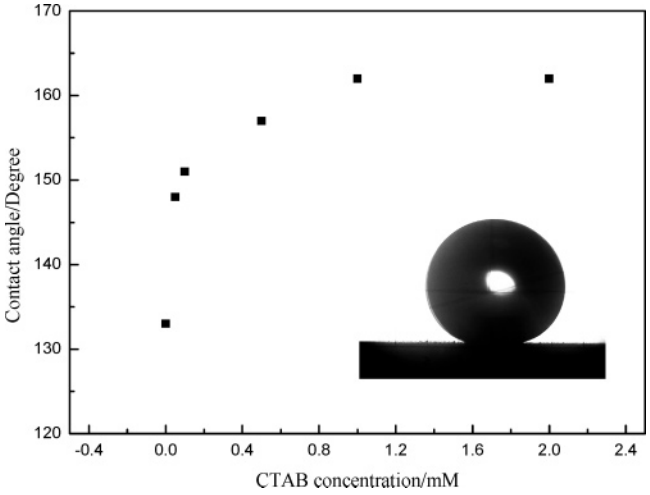

Figure 6. Water contact angle measurements of the surface of the porous copper films electrodeposited at a 0.8 A cm^{-2} cathodic current density for 85 s in the electrolyte of 0.04 M $CuSO_4$ + 0.5 M H_2SO_4 containing different CTAB concentration. The inset photo image shows the shape of a water droplet on the surface of the porous copper film with the maximum contact angle, which was electrodeposited at a 0.8 A cm^{-2} cathodic current density for 85 s in the electrolyte of 0.04 M $CuSO_4$ + 0.5 M H_2SO_4 + 2 mM CTAB.

thickness of the porous copper films did not change with the concentration of CTAB in solution. Because the pore size and wall thickness of the porous copper films are determined by the bubble size, it is clear that the bubble size is affect by the surfactant concentration. This phenomenon is in full agreement with the results reported previously by other researchers.[26−33]

The wettability of solid surfaces is governed by both the chemical composition and the geometrical microstructure of the surface.[34−40] Much of the recent research on hydrophobic materials has been inspired by the water-repellent nature of lotus leaves, which show a double roughness on their surfaces (nanohairs on microbumps) along with a waxy coating.[34] The hierarchical structures created by nanostructures on microstructures give a novel approach to constructing superhydrophobic surfaces as in the natural world. The as-prepared copper films with macropores and nanoparticles have a hierarchical structure. The porous copper films are made up of pores each 10 to 150 μm and composed of smaller (ca. 32 nm) faceted crystallites, showing a typical "double roughness" structure. These structures can induce superhydrophobic surfaces with large contact angle (CA), which has commonly been used as a criterion for the evaluation of hydrophobicity of a solid surface. We studied the effect of pore size of the porous copper film on the surface CA. The photographically measured contact angles of the copper films after treatment with *n*-hendecane thiol are shown in Figure 6. As shown in Figure 5, the pore sizes of electroposited copper films decrease with the increase in additive (CTAB) concentration. Along with pore size reduction, the CA of the porous copper films increases. When the pore size reached minimum, the copper film appeared the greatest contact angle (162°), showing a superhydropohobicity. Currently, superhydrophobic surfaces with water CA higher than 150° are arousing much interest because they will bring great progress. Various phenomena, such as snow sticking, contamination, or oxidation and current conduction, are expected to be inhibited on such a surface. The present work offers a simple and fast approach for preparing superhydrophobic surfaces.

Conclusion

We have synthesized macroporous copper films by using the gas bubble template-directed synthesis method. By this approach, hydrogen bubbles arising from the reduction of H^+ functioned as the dynamic template for copper electrodeposition. Copper was electrodeposited and grew within the interstitial spaces between the hydrogen bubbles, forming macroporous films on gold substrate. The porous copper films have open interconnected macroporous walls and nanoparticles and are self-supported structures. The pore size and wall thickness of the copper films could be tailored by varying the concentration of the electrodeposition electrolyte, the electrolyzing current density, and the concentration of surfactant (CTAB). The copper films with various pore size and wall thickness showing integrated microstructures and nanostructures offer a simple and fast means for fabricating surfaces with tunable superhydrophobicity.

Acknowledgment. This work was financially supported by the National Basic Research Program (2007CB936404), the National Natural Science Foundation of China (NSFC: 20535010), the National Science Fund for Creative Research Groups (20521503), and Natural Science Foundation of Jiangsu Province (BK2007147).

CM071738J

(39) Shi, F.; Song, Y. Y.; Niu, J.; Xia, X. H.; Wang, Z. Q.; Zhang, X. *Chem. Mater.* **2006**, *18*, 1365.
(40) Wang, C. H.; Song, Y. Y.; Zhao, J. W.; Xia, X. H. *Surf. Sci.* **2006**, *600*, L38.